626 Journal of Electrical Engineering & Technology Vol. 6, No. 5, pp. 626~633, 2011
http://dx.doi.org/10.5370/JEET.2011.6.5.626

A Study on Fast Maximum Efficiency Control of Stator-Flux-oriented Induction Motor Drives

Myoung-Ho Shin†

Abstract – This paper presents a novel maximum efficiency control scheme for convergence improvement in stator-flux-oriented induction motor drives. Three input powers are calculated at three different flux levels, respectively. A quadratic curve is obtained using the quadratic interpolation method using the three points. The flux level at the lowest point of the interpolated curve is calculated, which is not the real minimum input power of the motor, but an estimated one. Hence, the quadratic interpolations are repeated with three new points chosen using the selection method for new points for refitting until the convergence criteria are satisfied. The proposed method is verified by simulation results.

Keywords: Maximum efficiency control, Quadratic interpolation, Induction motor drive, Search controller

1. Introduction

Induction motors have been widely used in the industrial applications because of low cost, mechanical robustness, and simple maintenance. Many works for induction motors have been made recently [1]-[8].

Electric motors consume 50% of the total electric energy generated in the world. Induction motors are widely used in industries, and have the highest share in the electrical energy consumption among electric motors. Therefore, maximizing the efficiency of induction motor drives is important. The electric losses of a motor are mainly composed of copper and core losses. If copper loss increases, the core loss will decrease. There is a flux level at which motor input power is minimized for a given load torque and speed. Induction motors are highly efficient at rated loads with a rated flux. At light loads, however, the rated flux operation causes excessive core loss, thus impairing the efficiency of the motor. Therefore, a control technique that maximizes efficiency by adjusting the flux level is highly required at light loads [9]-[23].

There are two methods in obtaining the maximum efficiency operation for induction motors. The first is called Loss Model Controller (LMC) [11]-[14], in which losses are computed using the machine model. The flux level is then selected to minimize the losses. In [11], the optimal flux trajectories for vector control are proposed using the object function, which considers core and copper losses. In [12], the flux current is obtained using a loss-minimization algorithm, which minimizes the total loss from stator copper, rotor copper, and iron. Generally, convergence through the LMC method is considered fast, but is dependent on the induction motor parameters. Obtaining the exact motor parameters is difficult due to the parameter sensitivity to operating conditions [19].

The second method is the power-measure-based method known as search controller (SC) [15]-[21]. Online maximum efficiency control based on search is attractive. The flux is searched until the measured input power settles down to the lowest value for a given torque and speed. The control does not depend on any knowledge of induction motor parameters, and is insensitive to parameter variations.

In [15], a minimization method for input power by decreasing the flux reference in steps using a fixed value is proposed. However, the torque pulsation problem is unavoidable, and slow convergence is a major drawback. Studies on SCs are mainly focused on fast convergence. In [17], the squared rotor flux was adjusted using the Fibonacci search method until the measured input power reaches the minimum value. In [19], the golden section method was proposed to search the flux-producing current for the minimum measured input power for a given load torque and speed. The optimum point of flux is reached after nine iterations (1.8 s). In addition, the torque pulsation caused by the stepwise change in a flux-producing current is avoided using a low pass filter for the flux-producing current reference. Fuzzy [16], [20] and neuro-fuzzy [18] methods have been proposed to achieve convergence improvement. In [16], the optimum flux current reference was reached after six steps (2.5 s). In [20], the optimum point was obtained after 11 steps (5.5 s). Finally, in [18], the optimum flux was obtained after seven steps (about 10 s). The interpolation method was used in [21], but lacked an overall analysis.

In [22] and [23], a hybrid method combining the Loss

† Corresponding Author: Dept. of Electrical Engineering, Seoul National University of Science and Technology, Seoul, Korea. (mhshin@seoultech.ac.kr)
Received: July 13, 2010; Accepted: March 10, 2011

Model and the Search Method is proposed for convergence improvement. In [22], the first optimum flux was estimated using the LMC method. The subsequent flux adjustments were achieved using the SC method. The optimum flux current reference was obtained after five steps (1.2 s). However, the authors did not clearly present the current step for the SC method, which was adjusted adaptively. In [23], the operating point for the minimum loss was rapidly computed using a functional approximation of the motor and power converter losses. The loss function parameters were obtained from the measured input power. However, field orientation cannot be achieved in rotor-flux-oriented drive rotor resistance is detuned. All inputs for online loss parameter identification, as well as motor torque, might have errors attributed to field orientation errors due to the detuning of rotor resistance. In addition, the resulting algorithm is complex.

This paper proposes a convergence improvement method using a quadratic interpolation method. Three input powers are calculated for three flux levels. A quadratic curve is obtained using the quadratic interpolation method with the three points. The flux level at the lowest point of the interpolated curve is then calculated, which is not the real minimum input power of the motor, but an estimated one. Hence, quadratic interpolations are repeated with three new points chosen using the selection method for new points for refitting until the convergence criteria are satisfied. The proposed method is verified by simulation results.

2. Induction Motor Model with Core Loss

The synchronous reference frame *d-q* equivalent circuit of the induction motor is shown in Fig. 1, where the core loss is represented by a core-loss resistance.

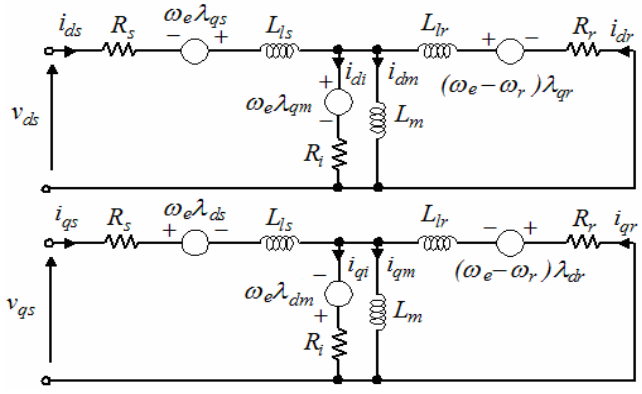

Fig. 1. Induction motor *d-q* equivalent circuit

The *d-q* equations of the three phases of the induction motor in the synchronous reference are expressed as follows [24]:

$$v_{ds} = R_s i_{ds} + p\lambda_{ds} - \omega_e\lambda_{qs} \quad (1)$$

$$v_{qs} = R_s i_{qs} + p\lambda_{qs} + \omega_e\lambda_{ds} \quad (2)$$

$$0 = R_r i_{dr} + p\lambda_{dr} - (\omega_e - \omega_r)\lambda_{qr} \quad (3)$$

$$0 = R_r i_{qr} + p\lambda_{qr} + (\omega_e - \omega_r)\lambda_{dr} \quad (4)$$

$$R_i i_{di} = p\lambda_{dm} - \omega_e\lambda_{qm} \quad (5)$$

$$R_i i_{qi} = p\lambda_{qm} + \omega_e\lambda_{dm} \quad (6)$$

$$T_e = \frac{3}{4}P_m(\lambda_{qr} i_{dr} - \lambda_{dr} i_{qr}) \quad (7)$$

$$i_{di} \approx \frac{-\omega_e}{R_i}(\lambda_{qs} - L_{ls} i_{qs}) \quad (8)$$

$$i_{qi} \approx \frac{\omega_e}{R_i}(\lambda_{ds} - L_{ls} i_{ds}) \quad (9)$$

where $p=d/dt$; R_s = stator resistance; R_r = rotor resistance; R_i = equivalent iron loss resistance; ω_e = excitation angular frequency; ω_r = rotor angular frequency; v_{ds}, v_{qs} = *d* and *q* axes stator voltages, respectively; i_{ds}, i_{qs} = *d* and *q* axes stator currents, respectively; i_{dr}, i_{qr} = *d* and *q* axes rotor currents, respectively; i_{di}, i_{qi} = *d* and *q* axes currents flowing through R_i, respectively; $\lambda_{ds}, \lambda_{qs}$ = *d* and *q* axes stator fluxes, respectively; $\lambda_{dm}, \lambda_{qm}$ = *d* and *q* axes air-gap fluxes, respectively; $\lambda_{dr}, \lambda_{qr}$ = *d* and *q* axes rotor fluxes, respectively; T_e = torque; and P_m = number of poles.

The induction motor losses consist of copper, iron, and stray losses [13]. Stray loss is mainly attributed to the rotor current. With regard to the EU requirements for 1.1–90 kW motors classified into EFF1–EFF3 groups according to their efficiency curves, the total secondary loss (stray flux, skin effect, and shaft stray losses) should not exceed 5% of the overall losses. Considering that stray losses are important at high loads and overload conditions, they are not considered as separate loss components in the loss modeling of the induction motor although the maximum efficiency control is effective at light loads [23]. Therefore, the total induction motor loss can be written as the sum of the stator copper, rotor copper, and iron losses [14].

$$P_l = \frac{3}{2}R_s(i_{ds}^2 + i_{qs}^2) + \frac{3}{2}R_r(i_{dr}^2 + i_{qr}^2) + \frac{3}{2}R_i(i_{di}^2 + i_{qi}^2) \quad (10)$$

The input power is the sum of the output power. The total induction motor loss can be expressed as (11):

$$P_d = P_l + P_{out} \quad (11)$$

where P_{out} is the output power of the motor.

3. Stator-Flux-oriented Control System

Fig. 2 shows the configuration of the maximum efficiency control for a stator-flux-oriented induction motor drive. The superscript ^ refers to the estimated variables

and quantities, and the superscript * denotes the reference variables and quantities.

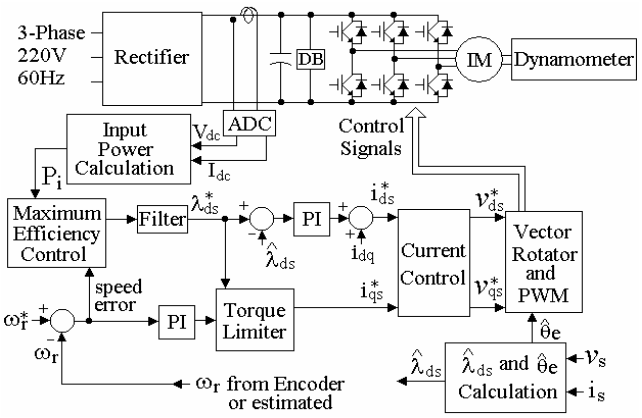

Fig. 2. Stator-flux-oriented control drive incorporating the proposed scheme

Stator flux can be estimated by integrating the back electromotive force as (12). Stator flux magnitude and transformation angle can be written as (13) and (14), respectively.

$$\vec{\hat{\lambda}}_s = \int (\vec{v}_s - R_s \vec{i}_s) dt \tag{12}$$

$$\left| \vec{\hat{\lambda}}_s \right| = \hat{\lambda}_{ds} = \sqrt{\hat{\lambda}_{\alpha s}^2 + \hat{\lambda}_{\beta s}^2} \tag{13}$$

$$\hat{\theta}_e = \tan^{-1} \frac{\hat{\lambda}_{\beta s}}{\hat{\lambda}_{\alpha s}} \tag{14}$$

where $\vec{\hat{\lambda}}_s$, $\hat{\lambda}_{\alpha s}$, $\hat{\lambda}_{\beta s}$, $\vec{v}_s$, $\vec{i}_s$ = stator flux vector, α–axis stator flux, β – axis stator flux, stator voltage vector, and stator current vector in stationary $\alpha - \beta$ reference frame, respectively.

The slip speed and the decoupling compensator can be represented in the rotating *d-q* reference frame as follows [24]:

$$\hat{\omega}_{sl} = \frac{L_s i_{qs} - L_m \hat{i}_{qi}}{\tau_r (\hat{\lambda}_{ds} - \sigma L_s i_{ds}) + \frac{L_{lr}}{R_r} L_m \hat{i}_{di}} \tag{15}$$

$$i_{dq} = \sigma \tau_r \hat{\omega}_{sl} i_{qs} + \frac{L_m}{L_s} (\hat{i}_{di} - \frac{\hat{\omega}_{sl} L_{lr} \hat{i}_{qi}}{R_r}) \tag{16}$$

where $\tau_r = L_r / R_r$ and $\sigma = 1 - L_m^2 / (L_s L_r)$.

The steady-state torque is given as [24]:

$$\hat{T}_e = \frac{3}{4} P_m [\hat{\lambda}_{ds} (i_{qs} - \hat{i}_{qi}) - L_{ls} (\hat{i}_{di} i_{qs} - \hat{i}_{qi} i_{ds})] \tag{17}$$

The stability condition of a stator-flux-oriented induction motor drive can be expressed as (18) [25]. In a "Torque Limiter" block, i_{qs}^* is limited by (18).

$$i_{qs}^* \le \frac{(1-\sigma)}{2\sigma L_s} \lambda_{ds}^* \tag{18}$$

The input power P_i can be calculated as the product of the inverter input voltage V_{dc} and the direct current I_{dc}.

$$P_i = V_{dc} I_{dc} \tag{19}$$

In the SC method, the input power of the induction motor is calculated by measuring the dc-link power P_i [15]-[21]. The flux is searched until the measured input power P_i settles down to the lowest value for a given torque and speed. The control method does not depend on any knowledge of the induction motor parameters, and is insensitive to parameter changes. P_i consists of copper, iron, and stray losses, as well as the switching loss of the inverter and the output power of the motor. P_d in (11) is almost the same as the P_i in (19) because switching and stray losses can be ignored. In the current study, P_d is used as the input motor power for the simulation.

The rotor speed is measured using an encoder. However, this step can be eliminated by speed estimation [26]. The load torque is applied to the motor by a dynamometer.

4. Proposed Maximum Efficiency Control

Fig. 3 shows an interpolated quadratic curve P_i, with three points (p_1, p_2, and p_3) obtained by measuring the input powers (P_{d1}, P_{d2}, and P_{d3}) at three given flux levels (λ_{ds1}, λ_{ds2}, and λ_{ds3}), respectively.

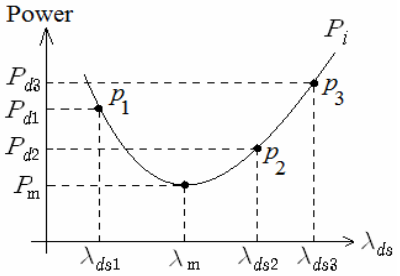

Fig. 3. Quadratic curve interpolated with three points p_1, p_2, and p_3.

The quadratic curve can be written as:

$$P_i = a + b\lambda_{ds} + c\lambda_{ds}^2 \tag{20}$$

The λ_m at the lowest point can be written as:

$$\lambda_m = -\frac{b}{2c} = \frac{P_{d1}(\lambda_{ds2}^2 - \lambda_{ds3}^2) + P_{d2}(\lambda_{ds3}^2 - \lambda_{ds1}^2) + P_{d3}(\lambda_{ds1}^2 - \lambda_{ds2}^2)}{2[P_{d1}(\lambda_{ds2} - \lambda_{ds3}) + P_{d2}(\lambda_{ds3} - \lambda_{ds1}) + P_{d3}(\lambda_{ds1} - \lambda_{ds2})]} \tag{21}$$

λ_m is the flux level obtained by the interpolated curve. The lowest power P_m is not the real input power of the motor. Therefore, the quadratic interpolations should be repeated until the given convergence criteria are satisfied. Table 1 shows the selection method of the three new points for the next quadratic interpolation [27].

Table 1. Selection of new points for refitting

Characteristics	New points for refitting
	New = Old
$\lambda_m < \lambda_{ds2}$ $P_m < P_{d2}$	$\lambda_{ds1} = \lambda_{ds1}$ $\lambda_{ds2} = \lambda_m$ $\lambda_{ds3} = \lambda_{ds2}$
$\lambda_m < \lambda_{ds2}$ $P_m > P_{d2}$	$\lambda_{ds1} = \lambda_m$ $\lambda_{ds2} = \lambda_{ds2}$ $\lambda_{ds3} = \lambda_{ds3}$
$\lambda_m > \lambda_{ds2}$ $P_m < P_{d2}$	$\lambda_{ds1} = \lambda_{ds2}$ $\lambda_{ds2} = \lambda_m$ $\lambda_{ds3} = \lambda_{ds3}$
$\lambda_m > \lambda_{ds2}$ $P_m > P_{d2}$	$\lambda_{ds1} = \lambda_{ds1}$ $\lambda_{ds2} = \lambda_{ds2}$ $\lambda_{ds3} = \lambda_m$

Eq. (22) determines if the convergence criterion is satisfied. The new flux level $\lambda_m(k+1)$ is compared with the present flux level $\lambda_m(k)$. If the difference is less than the convergence criterion of 0.008 Wb (2% of the rated flux level, 0.4 Wb), the quadratic interpolation is stopped, and $\lambda_m(k+1)$ becomes the final flux reference.

$$\left|\lambda_m(k+1)-\lambda_m(k)\right| < 0.008 \quad \text{Wb} \tag{22}$$

Torque pulsation might be produced because the flux reference is changed stepwise. To avoid torque pulsation, the low pass filter of (23) is used at the output of the "Maximum Efficiency Control" block in Fig. 2. Thus, the flux reference is smoothly changed.

$$G_1(s) = \frac{\alpha_1}{s+\alpha_1} \tag{23}$$

In [19], the input power was sampled and was averaged over a given period to measure the correct trend of the input of the driver. However, in this paper, the input power P_d is sampled every 125 μs and is filtered through a low pass filter as follows:

$$G_2(s) = \frac{\alpha_2}{s+\alpha_2} \tag{24}$$

If the speed reference is changed, the flux reference λ_{ds}^* is forced to have a rated value of 0.4 Wb to give the best transient responses. The activation of the maximum efficiency control routine is determined by the speed error ($\omega_r^* - \omega_r$). When the speed error becomes less than 2% of the speed reference, the maximum efficiency control routine is activated.

5. Simulation Results

The proposed scheme was verified by a simulation that used Advanced Continuous Simulation Language with the drive system shown in Fig. 2. The current control is executed every 125 μs. The flux and speed control are executed every 1.25 ms. The maximum efficiency control is executed every 375 ms. The "α_1" of the low pass filter in (23) has a value of 25. The input power P_d is calculated every 125 μs, and is filtered using a low pass filter. The "α_2" of the low pass filter in (24) is 300. The induction motor parameters are shown in Table 2.

Table 2. Induction motor parameters

3-phase, 5-hp, 220 (V), 4 (poles)	
Stator resistance	1.26 (Ω)
Rotor resistance	0.21 (Ω)
Magnetizing inductance	0.05 (H)
Stator leakage inductance	0.0047 (H)
Rotor leakage inductance	0.0047 (H)
Equivalent iron loss resistance	60 (Ω)

Fig. 4 shows that P_d, as the flux reference, decreases stepwise from 0.4 to 0.175 Wb by a fixed amount of 0.0008 Wb. With the given speed reference and load torque, the input power P_d is calculated at each flux reference, showing a lowest point of the input power. The lowest P_d is about 773 W at 0.242 Wb, which means the losses are minimized if the flux reference is 0.242 Wb at 1,300 rpm, and the load torque is 4 N·m.

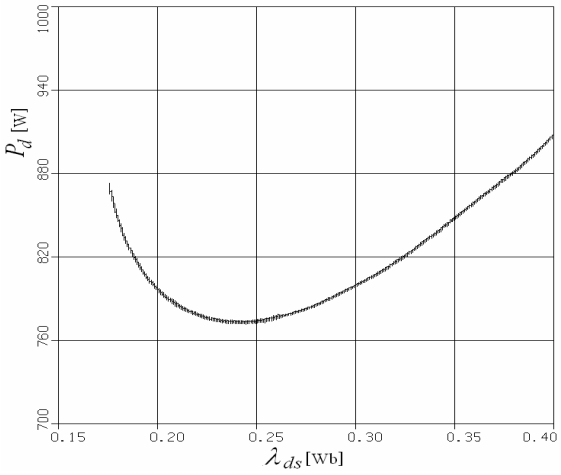

Fig. 4. P_d versus λ_{ds} at speed reference = 1,300 rpm and load torque = 4 N·m.

Fig. 5 shows the simulation results of the proposed maximum efficiency control. The speed reference is 1,300 rpm under a load torque of 4 N·m. The maximum efficiency control is activated at t = 3.375 s. The initial magnetic flux references for the quadratic interpolation are λ_{ds3} = 0.4 Wb, λ_{ds2} = 0.26 Wb, and λ_{ds1} = 0.22 Wb. λ_{ds3} is selected as the rated flux level of 0.4 Wb because the motor operates in transients at the rated flux level to give a rapid speed response. λ_{ds2} and λ_{ds1} are selected as arbitrary values considering the flux level at the lowest point of the curve in Fig. 4.

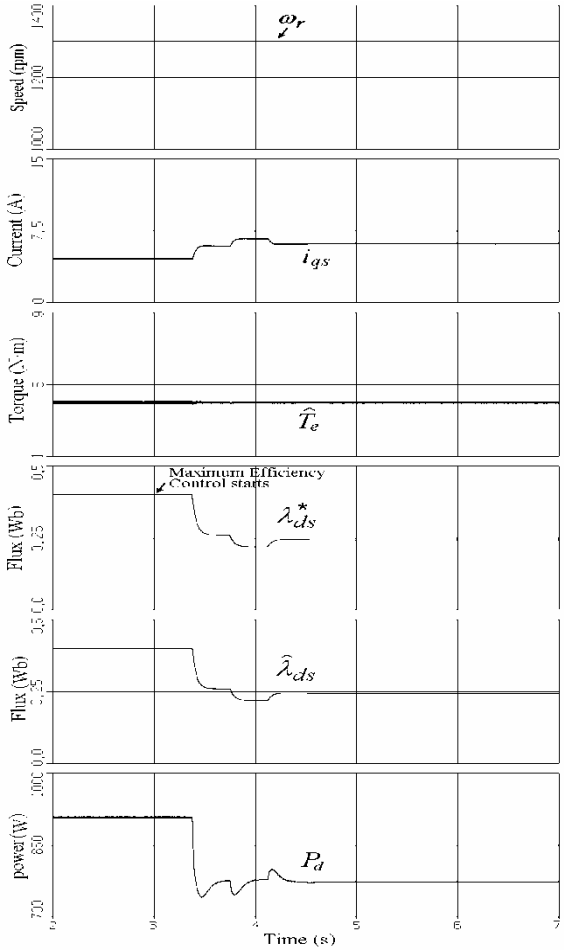

Fig. 5. Simulation results by the maximum efficiency control at speed reference = 1,300 rpm and load torque = 4 N·m

The calculated flux reference $\lambda_m(1)$ using the first quadratic interpolation is 0.245563 Wb. The next three flux references for the quadratic interpolation are λ_{ds3} = 0.26 Wb, λ_{ds2} = 0.245563 Wb, and λ_{ds1} = 0.22 Wb using the method for selecting new points for refitting in Table 1. The calculated flux reference $\lambda_m(2)$ using the second quadratic interpolation is 0.242346 Wb. The difference of $|\lambda_m(2)-\lambda_m(1)|$ is 0.003217 Wb, which is less than the convergence criterion of 0.008 Wb in (22). Therefore, the final flux reference is 0.242346 Wb. The torque remains nearly constant using the low pass filter of (23) for the flux reference. The optimum flux reference is obtained after four iterations (4 x 0.375 s = 1.5 s). Convergence improvement is achieved using the proposed method, as opposed to the most conventional methods (see the "Introduction" section).

Fig. 6 shows the P_d of Fig. 4, and P_i interpolated with three points at λ_{ds3} = 0.4 Wb, λ_{ds2} = 0.26 Wb, and λ_{ds1} = 0.22 Wb. Fig. 7 shows the P_d of Fig. 4 and P_i interpolated with three points at λ_{ds3} = 0.26 Wb, λ_{ds2} = 0.245563 Wb, and λ_{ds1} = 0.22 Wb. In Fig. 6, P_i has an error from 0.21 to 0.28 Wb, including the lowest point. In Fig. 7, however, P_i is almost the same as the P_d in the region from 0.21 to 0.28 Wb. The lowest point of P_d is searched by the proposed method.

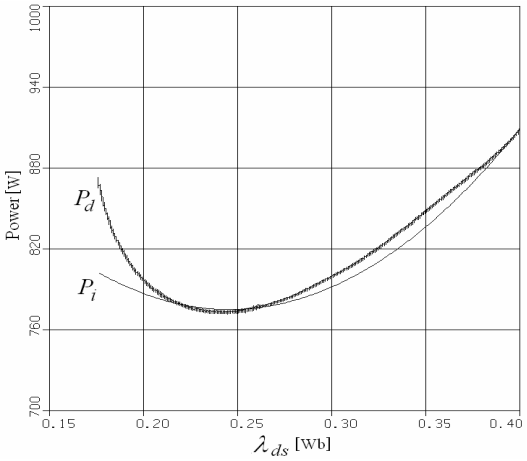

Fig. 6. P_d and P_i at speed reference = 1,300 rpm and load torque = 4 N·m (λ_{ds3} = 0.4 Wb, λ_{ds2} = 0.26 Wb, and λ_{ds1} = 0.22 Wb)

Fig. 8 shows the simulation results when the speed reference is changed from 1,300 to 1,700 rpm. In the proposed method, if the speed reference is changed, the flux level becomes its rated value of 0.4 Wb to provide fast transient responses. The flux level reaches its rated value of 0.4 Wb at the instant of the change of the speed reference. When the speed error becomes less than 2% of the speed reference, the maximum efficiency control routine is then activated. At a speed reference of 1,700 rpm and a load torque of 4 N·m, the first interpolation starts with the three points at λ_{ds3} = 0.4 Wb, λ_{ds2} = 0.26 Wb, and λ_{ds1} = 0.22 Wb. The calculated flux reference $\lambda_m(1)$ using the first interpolation is 0.210729 Wb. The next three flux references for the quadratic interpolation are selected as λ_{ds3} = 0.26 Wb, λ_{ds2} = 0.210729 Wb, and λ_{ds1} = 0.22 Wb using the selection method in Table 1. The calculated flux reference $\lambda_m(2)$ using the second quadratic interpolation is 0.22657 Wb. The difference $|\lambda_m(2)-\lambda_m(1)|$ is 0.015841 Wb, which is larger than the convergence criterion of 0.008 Wb. The next three flux references for the third

interpolation are selected as λ_{ds3} = 0.26 Wb, λ_{ds2} = 0.22657 Wb, and λ_{ds1} = 0.210729 Wb. The calculated flux reference $\lambda_m(3)$ using the third quadratic interpolation is 0.225541 Wb. The difference $|\lambda_m(3)-\lambda_m(2)|$ is 0.001029 Wb, which is less than the convergence criterion of 0.008 Wb. Therefore, the final flux reference is 0.225541 Wb. The maximum efficiency control is automatically executed by the proposed method when the speed reference is changed.

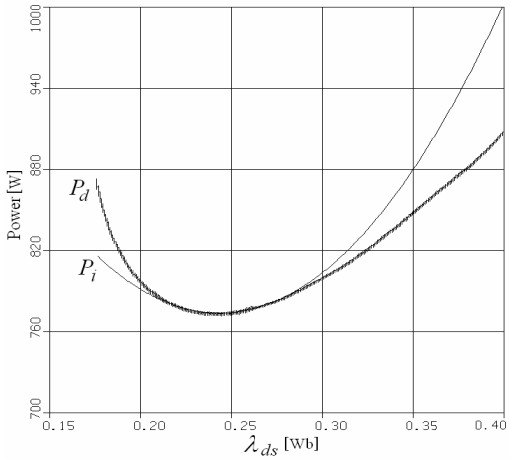

Fig. 7. P_d and P_i at a speed reference = 1,300 rpm and load torque = 4 N·m (λ_{ds3} = 0.26 Wb, λ_{ds2} = 0.245563 Wb, and λ_{ds1} = 0.22 Wb)

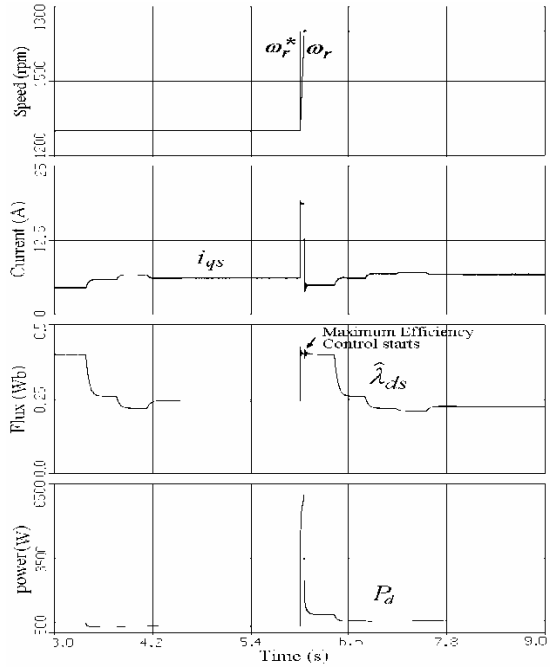

Fig. 8. Simulation results by the maximum efficiency control when the speed reference is changed from 1,300 to 1,700 rpm and load torque is 4 N·m

In Fig. 9, P_d is the input power as the flux reference decreases stepwise from 0.4 to 0.175 Wb by a fixed amount of 0.0008 Wb. The lowest P_d is about 992.4 W at 0.225 Wb. P_i is the interpolated curve with the three points at λ_{ds3} = 0.4 Wb, λ_{ds2} = 0.26 Wb, and λ_{ds1} = 0.22 Wb. Fig. 10 shows P_d and P_i interpolated with the three points at λ_{ds3} = 0.26 Wb, λ_{ds2} = 0.210729 Wb, and λ_{ds1} = 0.22 Wb. Fig. 11 shows P_d and P_i interpolated with the three points at λ_{ds3} = 0.26 Wb, λ_{ds2} = 0.22657 Wb, and λ_{ds1} = 0.210729 Wb. In Fig. 11, P_i is almost the same as the P_d in the region from 0.2 to 0.28 Wb, including the lowest point of P_d.

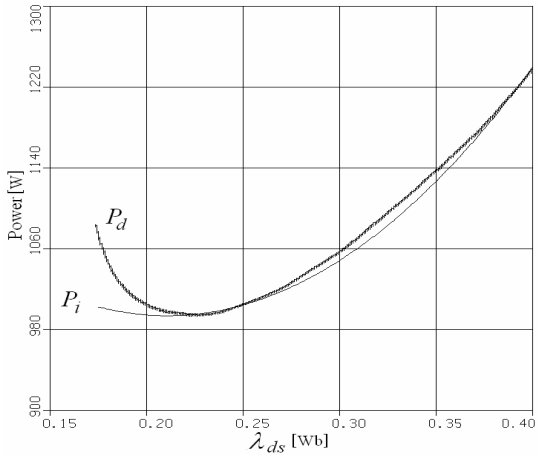

Fig. 9. P_d and P_i at speed reference = 1,700 rpm and load torque = 4 N·m (λ_{ds3} = 0.4 Wb, λ_{ds2} = 0.26 Wb, and λ_{ds1} = 0.22 Wb)

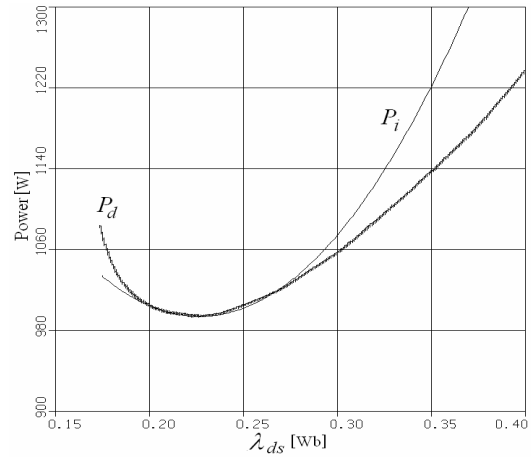

Fig. 10. P_d and P_i at speed reference = 1,700 rpm and load torque = 4 N·m (λ_{ds3} = 0.26 Wb, λ_{ds2} = 0.210729 Wb, and λ_{ds1} = 0.22 Wb)

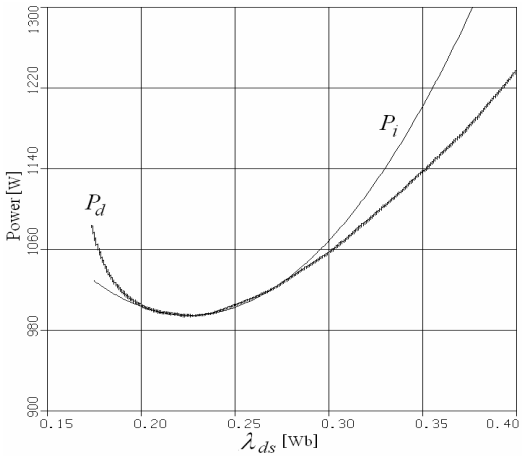

Fig. 11. P_d and P_i at speed reference = 1,700 rpm and load torque = 4 N·m (λ_{ds3} = 0.26 Wb, λ_{ds2} = 0.22657 Wb, and λ_{ds1} = 0.210729 Wb)

6. Conclusion

In the current study, a maximum efficiency control algorithm using a quadratic interpolation technique is proposed. The algorithm is used to search a flux level in which the input power reaches a minimum for a given torque and speed in a stator-flux-oriented induction motor drive. The torque pulsation caused by the stepwise change of the flux level is avoided using a low pass filter for the flux reference. In the simulation results, the proposed control algorithm achieved fast convergence to the lowest input power and torque ripple was avoided using a low pass filter for the flux reference.

References

[1] Hadda Benderradji,y, a maximum efficiency control algorithm∞ Theory based on Loopshapingmum efficiency control algorithm using a quadratic interpolation technique is proposed

[2] Hyung-Woo Lee, Chan-Bae Park, Byung-Song Lee, "Thrust Performance Improvement of a Linear Induction Motor" Journal of Electrical Engineering &Technology, Vol. 6, No. 1, pp.81-85, Jan. 2011.

[3] A.C. Megherbi, H. Megherbi, K. Benmahamed, A.G. Aissaoui, A. Tahour, "Parameter Identification of Induction Motors using Variable-weighted Cost Function of Genetic Algorithms" Journal of Electrical Engineering &Technology, Vol. 5, No. 4, pp.597-605, Nov. 2010.

[4] Ammar Medoued, Abdesselem Lebaroud, Ahcene Boukadoum, Guy Clerc, "On-line Faults Signature Monitoring Tool for Induction Motor Diagnosis" Journal of Electrical Engineering &Technology, Vol. 5, No. 1, pp.140-145, Mar. 2010.

[5] Seesak Jangjit, Panthep Laohachai, "Parameter Estimation of Three-Phase Induction Motor by Using Genetic Algorithm", Journal of Electrical Engineering &Technology, Vol. 4, No. 3, pp.360-364, Sep. 2009.

[6] Namhun Kim, Minhuei Kim, "Modified Direct Torque Control System of Five Phase Induction Motor" Journal of Electrical Engineering &Technology, Vol. 4, No. 2, pp.266-271, Jun. 2009.

[7] Abdessalem Chikhi, Khaled Chikhi, "Induction Motor Direct Torque Control with Fuzzy Logic Method" Journal of Electrical Engineering &Technology, Vol. 4, No. 2, pp.234-239, Jun. 2009.

[8] Arezki Menacer, Gérard Champenois, Mohamed Said Naît Saïd, Abdelhamid Benakcha, Sandrine Moreau, Said Hassaine, "Rotor Failures Diagnosis of Squirrel Cage Induction Motors with Different Supplying Sources", Journal of Electrical Engineering &Technology, Vol. 4, No. 2, pp.219-228, Jun. 2009.

[9] D. S. Krischen, D. W. Novotny, and W. Suwanwisoot, "Minimizing induction losses by excitation control in variable frequency drives," IEEE Trans. on Industry Applications, vol. 20, pp. 1244-1250, Sep./Oct. 1984.

[10] S.-K. Sul and M.-H. Park, "A novel technique for optimal efficiency control of a current-source inverter-fed induction motor", IEEE Trans. on Power Electronics, vol. 3, no. 2, pp. 192-199, 1988.

[11] R. D. Lorenz and S. M. Yang, "Efficiency-optimized flux trajectories for closed-cycle operation of field-orientation induction machine drives," IEEE Trans. on Industry Applications, vol. 28, pp. 574-580, May/June 1992.

[12] G. O. Garcia, J. C. Mendes Luis, R. M. Stephan, and E. H. Watanabe, "An efficient controller for an adjustable speed induction motor drive, " IEEE Trans. on Industrial Electronics, vol. 41, pp. 533-539, Oct. 1994.

[13] I. Kioskeridis and N. Margaris, "Loss minimization in induction motor adjustable-speed drive," IEEE Trans. on Industrial Electronics, vol. 43, pp. 226-231, Feb. 1996.

[14] G. Dong and O. Ojo, "Efficiency optimizing control of induction motor using natural variables," IEEE Trans. on Industrial Electronics, vol. 53, no. 6, pp. 1791-1798, Dec. 2006.

[15] D. S. Kirschen, D. W. Novotny, and T. A. Lipo, "On-line efficiency optimization of a variable frequency induction motor drive", IEEE Trans. on Industry Applications, vol. 21, no. 4, pp. 610-615, 1985.

[16] G. C. D. Sousa, B. K. Bose, and J. G. Cleland, "Fuzzy logic based on-line efficiency optimization control of an indirect vector-controlled induction motor drive", IEEE Trans. on Industrial Electronics, vol. 42, no. 2, pp. 192-198, 1995.

[17] G.-S. Kim, I.-J. Ha, and M.-S. Ko, "Control of induction motors for both high dynamic performance and high power efficiency", IEEE Trans. on Industrial Electronics, vol. 39, no. 4, pp. 323-333, 1992.

[18] B. K. Bose, N. R. Patel, and K. Rajashekara, "A Neuro-Fuzzy-Based On-Line Efficiency Optimization Control of a Stator Flux-Oriented Direct Vector-Controlled Induction Motor Drive", IEEE Trans. on Industrial Electronics, vol. 44, no. 2, pp. 270-273, 1997.

[19] C.-M. Ta and Y. Hori, "Convergence improvement of efficiency optimization control of induction motor drives", IEEE Trans. on Industry Applications, vol. 37, no. 6, pp. 1746-1753, 2001.

[20] D. D. A. Souza, W. C. P. D. A. Filho, and G. C. D. Sousa, "Adaptive fuzzy controller for efficiency optimization of induction motors," IEEE Trans. on Industrial Electronics, vol. 54, no. 4, pp. 2157-2164, Aug. 2007.

[21] M.-H. Shin, "Maximum efficiency control of induction motor drives using quadratic interpolation method", Journal of the Korean Institute of Illuminating and Electrical Installation Engineers, vol. 23, no.9, pp. 62-66, 2009.

[22] C. Chakraborty and Y. Hori, "Fast efficiency optimization techniques for the indirect vector-controlled induction motor drives", IEEE Trans. on Industry Applications, vol. 39, no. 4, pp. 1070-1076, 2003.

[23] S. N. Vukosavic and E. Levi, "Robust DSP-based efficiency optimization of a variable speed induction motor drive," IEEE Trans. on Industrial Electronics, vol. 50, no. 3, pp. 560-570, Jun. 2003.

[24] S.-D. Wee, M.-H. Shin, and D.-S. Hyun, "Stator-Flux-Oriented Control of Induction Motor Considering Iron Loss," IEEE Trans. on Industrial Electronics, vol. 48, no. 3, pp. 602-608, Jun. 2001.

[25] X. Xu, R. D. Doncker, and D. W. Novotny, "A Stator Flux Oriented Induction Machine Drive", IEEE PESC88, pp. 870-876, 1988.

[26] X. Xu and D. W. Novotny, "Implementation of direct stator flux orientation control on a versatile DSP based system," IEEE Trans. Ind. Applications, vol. 27, no. 4, pp. 694–700, July/Aug. 1991.

[27] S. S. Rao, "Optimization: Theory and Applications," John Willy and Sons, pp.234-242, 1984.

Myoung-Ho Shin received his B.S., M.S., and Ph.D. degrees in electrical engineering from Hanyang University, Seoul, Korea, in 1989, 1991, and 2001, respectively. From 1991 to 1996, he was with Samsung Advanced Institute of Technology, Suwon, Korea, as a senior researcher. He is currently with Seoul National University of Science and Technology, Seoul, Korea, where he is an associate professor in the Department of Electrical Engineering. His research interests include electrical machines and control systems.